A Family of Large-Stencil Discrete Laplacian Approximations in Three Dimensions

Randall C. O'Reilly

University of Colorado Boulder
345 UCB
Boulder, CO 80309
Randy.OReilly@colorado.edu
(Dated: June 11, 2006)

A family discrete approximations to the Laplacian operator with increasingly large stencil sizes for explicit-Euler integration is derived and analyzed. This family includes a 19-point stencil described earlier by Barkley and colleagues, and a new 27-point stencil. This 27-point stencil, which includes all 26 adjacent neighbors in a face-centered regular cubic tiling of three-dimensional space (faces, edges, and corners), has a maximum stable time step parameter Δt_{max} of .5 for the first-order diffusion equation (and 1 for the second-order wave equation). In contrast, the standard 7-point stencil has a first-order $\Delta t_{max} = .166\overline{6}$ and the 19-point stencil $\Delta t_{max} = .375$. In addition to enabling faster computation, the larger neighborhood stencils also exhibit significantly greater rotational symmetry than the standard approximation.

I. INTRODUCTION

The Laplacian operator ∇^2 is the critical computation in several important equations, including the wave and diffusion equations, which occur widely across every branch of physics. To simulate waves in three dimensions on a computer, a three-dimensional discrete approximation is required. The standard approximation for explicit-Euler integration with a regular face-centered cubic tiling of space uses a 7-point stencil involving the central point and its 6 nearest neighbors along adjacent faces. A 19-point stencil that includes the 6 adjacent faces and the 12 next-nearest edge neighbors was described by Barkley and colleagues [1], which has two key advantages: a maximum stable time step that is 2.25 times larger than the 7-point case, and a significant reduction of grid anisotropies because the leading contributions to error are invariant under rotations. Here, we describe an even larger 27-point stencil that includes the 8 corner neighbors in addition to faces and edges, and has an even larger maximum stable time step ($1.33\overline{3}$ times larger than the 19-point, and 3 times larger than the 7-point), and improved rotational invariance.

II. DERIVATION OF THE 19-POINT STENCIL

The Laplacian is the divergence of the gradient:

$$\nabla^2 \equiv \vec{\nabla} \cdot \vec{\nabla} \equiv \frac{\partial^2}{\partial x^2} + \frac{\partial^2}{\partial y^2} + \frac{\partial^2}{\partial z^2}, \tag{1}$$

which appears in the standard second-order wave equation:

$$\frac{\partial^2 \varphi}{\partial t^2} = c^2 \nabla^2 \varphi, \tag{2}$$

where $0 < c < 1$ controls the speed of wave propagation.

For a discrete one-dimensional field φ_i with grid spacing h, the second spatial derivatives can be ap-

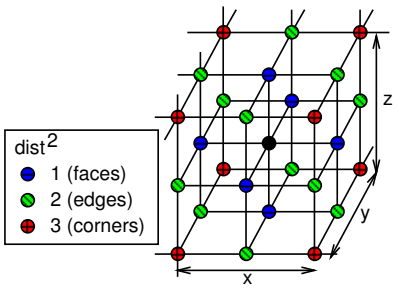

Figure 1: Face-centered cubic tiling of space, showing centers of cells as nodes, with all 26 neighbors of a given cell shown. The standard discrete approximation uses only the 6 face neighbors. Other approximations here enable all 26 to be used.

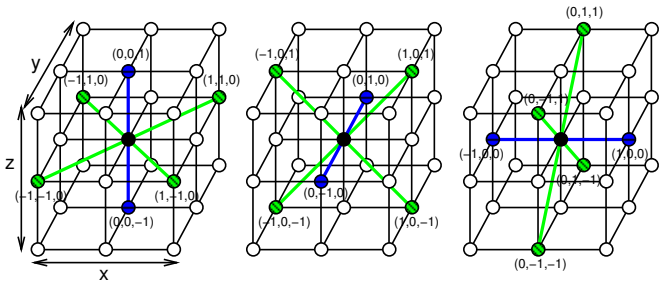

Figure 2: Three sets of orthogonal axes involving faces and edges, which includes all 18 of these neighbors, with no overlap across sets. A more stable 19-point stencil approximation to the Laplacian can be constructed by averaging across these sets.

proximated by taking the difference of two first order difference equations:

$$\frac{\partial \varphi}{\partial x} \approx D^{-}\varphi_i = \frac{1}{h}(\varphi_i - \varphi_{i-1}) \tag{3}$$

$$\approx D^{+}\varphi_i = \frac{1}{h}(\varphi_{i+1} - \varphi_i) \tag{4}$$

$$\frac{\partial^2 \varphi}{\partial x^2} \approx \frac{1}{h}(D^{+}\varphi_i - D^{-}\varphi_i) = \frac{1}{h^2}(\varphi_{i+1} + \varphi_{i-1} - 2\varphi_i). \tag{5}$$

In a discretized three-dimensional space using a face-centered cubic tiling (Figure 1, grid spacing h), the standard approximation is to simply apply the one-dimensional discretization to each of the three axes, using the 6 face neighbors:

$$\begin{aligned}
\nabla_f^2 \varphi_i &= \frac{1}{h^2}\left(\varphi_{(1,0,0)} + \varphi_{(-1,0,0)} + \varphi_{(0,1,0)} + \varphi_{(0,-1,0)} + \varphi_{(0,0,1)} + \varphi_{(0,0,-1)} - 6\varphi_i\right) \\
&= \frac{1}{h^2}\sum_{j \in \mathcal{N}_f} \varphi_j - 6\varphi_i \\
&= \frac{1}{h^2}\sum_{j \in \mathcal{N}_f} (\varphi_j - \varphi_i),
\end{aligned} \tag{6}$$

where ∇_f^2 denotes the face-based approximation and $\varphi_{(x,y,z)}$ indicates the neighbor at the given (x, y, z) offset from the point being computed (φ_i). This set of 6 neighbors is denoted $\mathcal{N}_f$ (faces). The final form shows that each neighbor contributes the difference between its value and the central value to the overall sum.

A problem with this standard approximation is that, in the wave equation, many of the neighboring points in space are not directly affected by a disturbance propagating along a non-cartesian axis, because a given cell is only influenced by this small subset of neighbors. This introduces preferred directions of wave propagation (anisotropy), and also leads to numerical instability.

One strategy for including a larger set of neighbors in the Laplacian calculation is to construct three new orthogonal basis sets from the face and edge points, as shown in Figure 2. Each set of neighbors has no overlap with the others, and together they include all of the face and edge points. Therefore, we can include all of the face and edge neighbors by averaging across these three basis cases:

$$\begin{aligned}
\nabla^2_{fe}\varphi_i &= \frac{1}{3h^2}\left(\sum_{j\in\mathcal{N}_f}(\varphi_j-\varphi_i)+\frac{1}{2}\sum_{j\in\mathcal{N}_e}(\varphi_j-\varphi_i)\right) \\
&= \frac{1}{3h^2}\left(\sum_{j\in\mathcal{N}_f}\varphi_j+\frac{1}{2}\sum_{j\in\mathcal{N}_e}\varphi_j-12\varphi_i\right) \\
&= \frac{1}{6h^2}\left(2\sum_{j\in\mathcal{N}_f}\varphi_j+\sum_{j\in\mathcal{N}_e}\varphi_j-24\varphi_i\right) \qquad (7)
\end{aligned}$$

where the $\frac{1}{3}$ factor comes from the averaging of the three basis sets, and the $\frac{1}{2}$ factor for the edges reflects a normalization by the distance to the edge neighbors. The last form shown above is equivalent to the 19-point stencil (18 neighbors = 6 faces + 12 edges) derived by Barkley and colleagues [1].

III. STABILITY ANALYSIS OF THE 19-POINT STENCIL

We reproduce here the stability analysis (in slightly more detail) of the 19-point stencil as performed by Barkley and colleagues [1], which we will extend to the 27-point case later. The overall strategy is to perform an eigenvalue analysis, where stability requires that the largest eigenvalue have a magnitude of less than 1.

First, the first-order diffusion equation is considered, because it is simpler to analyze than the second-order wave equation (the maximum stable time step for the second order equation is twice that of this first order one):

$$\frac{\partial u}{\partial t}=\nabla^2 u. \qquad (8)$$

Using the 19-point faces + edges approximation and explicit-Euler time stepping, this is:

$$\begin{aligned}
u_i^{n+1} &= u_i^n+\Delta t\nabla^2_{fe} \\
&= u_i^n+\Delta t\frac{1}{3h^2}\left(\sum_{j\in\mathcal{N}_f}u_j^n+\frac{1}{2}\sum_{j\in\mathcal{N}_e}u_j^n-12u_i^n\right). \qquad (9)
\end{aligned}$$

This can be expressed as a linear equation:

$$u_{ijk}^{n+1}=\mathbf{A}u_{ijk}^n, \qquad (10)$$

where the matrix $\mathbf{A}$ contains the neighborhood weighting factors:

$$\mathbf{A}=1+\nabla^2_{fe}. \qquad (11)$$

This linear equation can be expressed in terms of eigenvalues λ operating on a rotated eigenfunction representation of the state values, ψ:

$$\mathbf{A}\psi_{ijk} = \lambda\psi_{ijk}. \tag{12}$$

The system is stable as long as all eigenvalues λ of the matrix $\mathbf{A}$ have a magnitude 1 or less. The eigenfunctions of $\mathbf{A}$ are discrete forms of the eigenfunctions of the Laplacian:

$$\psi_{ijk} = cos(l_x i)cos(l_y j)cos(l_z k), \tag{13}$$

where l_x, l_y, l_z are wavenumbers, and sine can replace any of the cosines as well.

To determine these eigenvalues, we write out all the terms of $\mathbf{A}$ and λ, and then derive a condensed expression. First, we set:

$$\epsilon = \frac{\Delta t}{3h^2} \tag{14}$$

and write $\mathbf{A}$ for each of the x, z planes along the different slices of $y = \{-1, 0, 1\}$:

$$\begin{aligned}
\mathbf{A}_{y=-1} &= \begin{pmatrix} 0 & \frac{\epsilon}{2} & 0 \\ \frac{\epsilon}{2} & \epsilon & \frac{\epsilon}{2} \\ 0 & \frac{\epsilon}{2} & 0 \end{pmatrix} \\
\mathbf{A}_{y=0} &= \begin{pmatrix} \frac{\epsilon}{2} & \epsilon & \frac{\epsilon}{2} \\ \epsilon & 1-12\epsilon & \epsilon \\ \frac{\epsilon}{2} & \epsilon & \frac{\epsilon}{2} \end{pmatrix} \\
\mathbf{A}_{y=+1} &= \begin{pmatrix} 0 & \frac{\epsilon}{2} & 0 \\ \frac{\epsilon}{2} & \epsilon & \frac{\epsilon}{2} \\ 0 & \frac{\epsilon}{2} & 0 \end{pmatrix}.
\end{aligned} \tag{15}$$

Substituting in the Laplacian eigenfunctions (13), this is:

$$\begin{aligned}
\lambda_{y=-1} &= \begin{pmatrix} 0 & \frac{\epsilon}{2}\cos(-l_y)\cos(l_z) & 0 \\ \frac{\epsilon}{2}\cos(-l_x)\cos(-l_y) & \epsilon\cos(-l_y) & \frac{\epsilon}{2}\cos(l_x)\cos(-l_y) \\ 0 & \frac{\epsilon}{2}\cos(-l_y)\cos(-l_z) & 0 \end{pmatrix} \\
\lambda_{y=0} &= \begin{pmatrix} \frac{\epsilon}{2}\cos(-l_x)\cos(l_z) & \epsilon\cos(l_z) & \frac{\epsilon}{2}\cos(l_x)\cos(l_z) \\ \epsilon\cos(-l_x) & 1-12\epsilon & \epsilon\cos(l_x) \\ \frac{\epsilon}{2}\cos(-l_x)\cos(-l_z) & \epsilon\cos(-l_z) & \frac{\epsilon}{2}\cos(l_x)\cos(-l_z) \end{pmatrix} \\
\lambda_{y=+1} &= \begin{pmatrix} 0 & \frac{\epsilon}{2}\cos(l_y)\cos(l_z) & 0 \\ \frac{\epsilon}{2}\cos(-l_x)\cos(l_y) & \epsilon\cos(l_y) & \frac{\epsilon}{2}\cos(l_x)\cos(l_y) \\ 0 & \frac{\epsilon}{2}\cos(l_y)\cos(-l_z) & 0 \end{pmatrix}.
\end{aligned} \tag{16}$$

Because cosine is symmetric about zero ($\cos(-l_x) = \cos(l_x)$), we can group like terms and get:

$$\begin{aligned}
\lambda \; = 1 + 2\epsilon \; &[\cos(l_x) + \cos(l_y) + \cos(l_z) + \\
&\cos(l_x)\cos(l_y) + \cos(l_y)\cos(l_z) + \cos(l_x)\cos(l_z) - 6].
\end{aligned} \tag{17}$$

The term inside the brackets has its largest magnitude at a value of -8, which occurs when any two of the wavenumbers are π and the third is 0 (otherwise it is -6). Thus, the overall largest magnitude eigenvalue is:

$$\lambda_{max} = 1 - \frac{16\Delta t}{3h^2}, \tag{18}$$

which means that the limiting Δt value required to keep $|\lambda_{max}| < 1$ is:

$$\Delta t_{max} = \frac{3}{8}h^2 = .375h^2. \tag{19}$$

Compare this with the corresponding value for the standard 7-point face-only stencil:

$$\Delta t_{max} = \frac{1}{6}h^2 = .166\overline{6}h^2. \tag{20}$$

Thus, the 19-point stencil can be run 2.25 times faster than the 7-point case.

IV. EXTENSION TO THE 27-POINT STENCIL

Although better than the 7-point stencil, the 19-point face + edge approximation still leaves out 8 of the neighbors: the corners. These are tricky because they do not form an orthogonal basis. Nevertheless, we can construct a stencil that includes them (a 27-point stencil) by noting that in the 19-point case, each neighbor contributes according to the following equation:

$$\frac{1}{||j-i||}(\varphi_j - \varphi_i), \tag{21}$$

where $||j-i||$ is the squared distance between the neighbor point j and the central point i (i.e., 1 for faces, 2 for edges, and 3 for corners). Furthermore, the sum is normalized by:

$$\frac{6}{N_{points}h^2}. \tag{22}$$

The 6 in the numerator comes from the fact that the canonical face-based Laplacian consists of 6 neighbor points located at the ends of the 3 rays that define the three second derivatives $\left(\frac{\partial^2\varphi}{\partial x^2} + \frac{\partial^2\varphi}{\partial y^2} + \frac{\partial^2\varphi}{\partial z^2}\right)$, which is then divided by the total number of points included in the sum (N_{points}; note that this the number of neighbors, excluding the central point).

These equations can be used to define a whole family of Laplacians involving various combinations of the faces, edges and corners, including faces only (7-point stencil; equation 6), faces + edges (19-point stencil; equation 7), and faces + edges + corners (27-point stencil):

$$\begin{aligned}\nabla^2_{fec}\varphi_i &= \frac{3}{13h^2}\left(\sum_{j\in\mathcal{N}_f}(\varphi_j-\varphi_i) + \frac{1}{2}\sum_{j\in\mathcal{N}_e}(\varphi_j-\varphi_i) + \frac{1}{3}\sum_{j\in\mathcal{N}_c}(\varphi_j-\varphi_i)\right)\\ &= \frac{3}{13h^2}\left(\sum_{j\in\mathcal{N}_f}\varphi_j + \frac{1}{2}\sum_{j\in\mathcal{N}_e}\varphi_j + \frac{1}{3}\sum_{j\in\mathcal{N}_c}\varphi_j - \frac{44}{3}\varphi_i\right)\end{aligned} \tag{23}$$

(see the Appendix for another derivation based on including additional neighbors in the first order gradient computation that also yields equation 23).

A. Stability Analysis of the 27-point Stencil

Applying the eigenvalue stability analysis from the 19-point case to this 27-point stencil, the λ matrix just adds 8 new terms for the corners, each of the form: $\frac{\epsilon}{3}\cos(\pm l_x)\cos(\pm l_y)\cos(\pm l_z)$, where the ϵ factor is now:

$$\epsilon = \frac{3\Delta t}{13h^2}. \tag{24}$$

Because of the cosine symmetry, the resulting eigenvalue equation includes just one additional term for the 8 corner factors, and the subtraction value for the central point is different:

$$\begin{aligned}\lambda \ = 1 + 2\epsilon \ & [\cos(l_x) + \cos(l_y) + \cos(l_z) + \\ & \cos(l_x)\cos(l_y) + \cos(l_y)\cos(l_z) + \cos(l_x)\cos(l_z) + \\ & \frac{4}{3}\cos(l_x)\cos(l_y)\cos(l_z) - \frac{22}{3}\Big]. \end{aligned} \tag{25}$$

The term inside the brackets has its largest magnitude at a value of $-8.66\overline{6}$, which occurs when the wavenumbers for all dimensions are π, and when only one wavenumber is π and the others are 0. Otherwise, this expression has a value of -8. Thus, the overall largest magnitude eigenvalue is:

$$\lambda_{max} = 1 - \frac{52\Delta t}{13h^2}, \tag{26}$$

which means that the limiting Δt value required to keep $|\lambda_{max}| < 1$ is:

$$\Delta t_{max} = \frac{13}{26}h^2 = .5h^2 \tag{27}$$

This is $1.33\overline{3}$ times larger than the Δt_{max} for the 19-point case, and 3 times larger than for the 7-point case.

For the second-order wave equation, where the maximum time step is twice that of the first-order diffusion equation, this means that $\Delta t_{max} = 1h^2$. It may be that this represents the largest time step possible for a nearest-neighbor explicit Euler integration method.

One can make a further observation about relative rotational symmetry as a function of stencil size, by comparing the magnitudes of maximal eigenvalues along different axes through the central point. For the 19 point case, there are only two maximal eigenvalues through the different axes, of magnitude 6 and 8, or a ratio of .75. In the 27 point case, these values are $8.66\overline{6}$ and 8, or a ratio of .923. Thus, the 27 point case has greater symmetry in these maximal eigenvalues along different rotational axes, suggesting that it has greater overall rotational symmetry.

V. CONCLUSION

The above analytical results were confirmed in numerical simulations of both the diffusion and wave equations. As argued by Barkley and colleagues [1], the small increase in computational cost required to include larger numbers of neighbors in the Laplacian is more than offset by the increase in maximal time step that these larger stencils afford. Accordingly, it would seem that the 27-point stencil should provide the most stable, rotationally symmetric, and efficient method for computing the Laplacian.

VI. APPENDIX: DISCRETE GRADIENTS WITH NEIGHBOR AVERAGING

The 27-point stencil can also be derived by way of a first-order gradient computation that uses more than the standard cartesian axis neighbors. The standard discrete gradient computation in one dimension involves averaging the two difference equations on either side of the point in question:

$$\begin{aligned} D^-\varphi_i \ &= \ \frac{1}{h}(\varphi_i - \varphi_{i-1}) \\ D^+\varphi_i \ &= \ \frac{1}{h}(\varphi_{i+1} - \varphi_i) \\ \frac{\partial\varphi}{\partial x} \approx \frac{1}{2}(D^+\varphi_i + D^-\varphi_i) \ &= \ \frac{1}{2h}(\varphi_{i+1} - \varphi_{i-1}) \end{aligned} \tag{28}$$

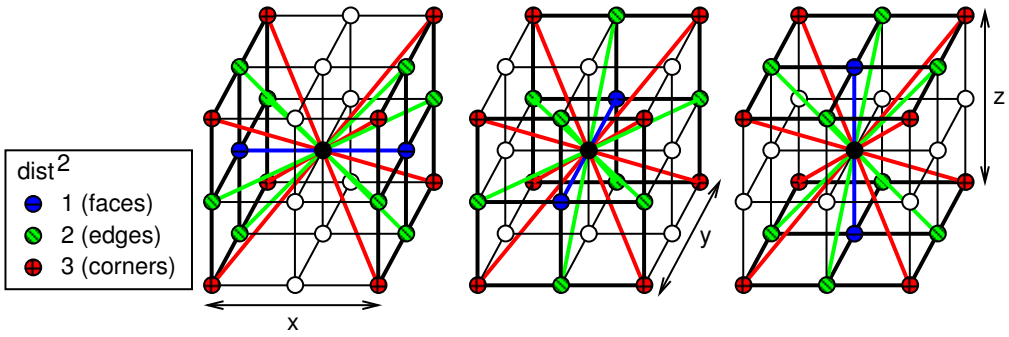

Figure 3: Computation of the first order spatial gradient using all 18 neighbors that have a non-zero projection along a given axis. Each neighbor contributes to the gradient in proportion with its projection along the axis (1 for face points, $\frac{1}{\sqrt{2}}$ for edges, and $\frac{1}{\sqrt{3}}$ for corners. Note that, across all three cases, the faces occur once, edges occur twice, and corners in all three cases (i.e., in proportion to their respective distances).

In three dimensions, the averaging process can be taken further by including rays through all neighboring points that have some projection along the gradient axis (Figure 3), with the contribution of each neighbor pair weighted by the extent of its projection along the axis:

$$\frac{\partial \varphi}{\partial x} \approx \frac{1}{h(2+\frac{8}{\sqrt{2}}+\frac{8}{\sqrt{3}})}\Big(\; (\varphi_{(1,0,0)} - \varphi_{(-1,0,0)}) + \\ \frac{1}{\sqrt{2}} \sum_{j \in \mathcal{N}_e} (\varphi_{j+} - \varphi_{j-}) + \frac{1}{\sqrt{3}} \sum_{j \in \mathcal{N}_c} (\varphi_{j+} - \varphi_{j-}) \Big) \tag{29}$$

where the neighborhoods $\mathcal{N}_e$ and $\mathcal{N}_c$ denote pairs of points $j+$ and $j-$ along the 4 rays through the edges and corners, respectively. The normalizing factor ensures that the weighted average sums to one.

Plugging this first-order gradient into the second-order difference-of-differences equation results in:

$$\frac{\partial^2 \varphi}{\partial x^2} \approx \frac{1}{h^2(1+\frac{4}{2}+\frac{4}{3})}\Big(\; (\varphi_{(1,0,0)} + \varphi_{(-1,0,0)} - 2\varphi_i) + \\ \frac{1}{2} \sum_{j \in \mathcal{N}_e} (\varphi_{j+} + \varphi_{j-} - 2\varphi_i) + \frac{1}{3} \sum_{j \in \mathcal{N}_c} (\varphi_{j+} + \varphi_{j-} - 2\varphi_i) \Big) \tag{30}$$

Which can be simplified by using sums over the individual neighbor points, instead of considering the rays:

$$\frac{\partial^2 \varphi}{\partial x^2} \approx \frac{3}{h^2 13} \left(\sum_{j \in \mathcal{N}_f} (\varphi_j - \varphi_i) + \frac{1}{2} \sum_{j \in \mathcal{N}_e} (\varphi_j - \varphi_i) + \frac{1}{3} \sum_{j \in \mathcal{N}_c} (\varphi_j - \varphi_i) \right) \tag{31}$$

We can then compute the Laplacian by summing together the derivatives along the three axes computed according to equation 31. However, the neighborhood of points involved for computing the derivatives along each axis overlaps partially with the others, as shown in Figure 3. Interestingly, this overlap is different depending on the distance of the neighbor, in exact proportion to this distance: faces appear once, edges appear twice, and corners appear three times. Thus, if one were to combine all the terms in the sums into a single computation operating across all the neighbors, this differential repetition of neighbors would exactly cancel out the distance-based normalization factors ($\frac{1}{2}$, $\frac{1}{3}$). However, it does not make sense to overcount the influence of some neighbors versus others. Therefore, we can simply drop the repeated factors from the equation, which then includes all of the 26 neighbors exactly once, and one arrives at equation 23. It is

interesting to note that both approaches arrive at the same $\frac{3}{13}$ normalization factor, via somewhat different routes.

---

[1] M. Dowle, R. M. Mantel, and D. Barkley, International Journal of Bifurcation and Chaos **7**, 2529 (1997).